

Exploring the Nonlinear Relationships Between Oceanic Indices Using Quantum and Classical Machine Learning Approaches

Swarna M^{1*}., Sudhakar N².,

¹Research Scholar, Acharya Nagarjuna University, Vijayawada, India

²Professor, Bapatla Engineering College, Bapatla, India

*corresponding author: swarnamkt@gmail.com

Abstract:

Understanding the complex interrelationships between oceanic climate indices such as the Indian Ocean Dipole (IOD), El Niño–Southern Oscillation (ENSO), Arctic Oscillation (AO), and Atlantic Multidecadal Oscillation (AMO) is crucial for improving long-term climate predictions. However, traditional linear models often fail to capture the intricate, nonlinear dependencies that govern these systems. As a result, these models struggle to accurately predict key oceanic anomalies and associated climatic events, such as tropical cyclones that significantly impact India and its surrounding regions.

In this study, we investigate both classical and quantum machine learning approaches to analyze the nonlinear interconnections among the four major oceanic indices. Using Random Forests and Mutual Information, we identify influencing relationships beyond what is revealed by linear correlation. To enhance interpretability and model generalization, we employ symbolic regression (via PySR) to derive analytical expressions that define the interactions among the indices. Our findings reveal hidden nonlinear influences—particularly highlighting that while AMO appears to have minimal effect under linear analysis, it plays a more subtle but critical role in the broader climate system.

By combining symbolic and quantum machine learning techniques, this research offers a novel, interpretable framework for understanding complex ocean-atmosphere dynamics and lays the groundwork for improved forecasting of extreme weather events such as tropical cyclones in the Indian subcontinent.

Keywords: Ocean Indices, tropical cyclones, Quantum computing, machine learning, statistical methods.

INTRODUCTION

The Earth's climate system is driven by a complex network of interacting oceanic and atmospheric phenomena. Among the most influential of these are large-scale oscillatory patterns such as the Indian Ocean Dipole (IOD), El Niño–Southern Oscillation (ENSO), Arctic Oscillation (AO), and Atlantic Multidecadal Oscillation (AMO). Each of these indices reflects a distinct pattern of ocean-atmosphere variability, and their individual and combined effects can significantly influence global and regional climate behavior.

Understanding the causal relationships and interdependencies among these indices is vital for improving forecasts of extreme climatic events. In particular, regions such as the Indian subcontinent are highly sensitive to these dynamics, where changes in oceanic conditions can strongly impact the frequency and intensity of tropical cyclones, monsoon variability, and other high-impact weather phenomena. Despite this importance, predictive capabilities remain limited, primarily due to the oversimplified nature of traditional statistical and linear models.

While linear correlation and regression methods have historically served as tools for analyzing these indices, they often fail to detect underlying nonlinear relationships. For instance, the Atlantic Multidecadal Oscillation (AMO) is frequently observed to exhibit weak linear influence on other indices. However, theoretical evidence and observational studies suggest that AMO may exert nonlinear effects, particularly over longer temporal scales. This discrepancy points to a need for more sophisticated modeling techniques capable of unveiling hidden patterns within the data.

To address these challenges, this study explores both classical and quantum machine learning (QML) approaches to investigate the nonlinear relationships between IOD, ENSO, AO, and AMO. In particular, we employ Random Forest regressors and Mutual Information to initially assess nonlinear dependencies, and further extend our analysis using Symbolic Regression via PySR—a powerful tool that allows us to generate explicit analytical expressions capturing these relationships.

Moreover, to evaluate the potential of quantum-enhanced learning, we leverage variational quantum circuits and hybrid quantum-classical models (using PennyLane) to model these dependencies. By comparing classical and quantum approaches, this study aims to both uncover the hidden structure among climate indices and propose an interpretable and scalable framework for future climate predictions.

RELATED WORK

Sea Surface temperature observations are important to understand the relationship between ocean and earth. The behaviour of ocean currents deeply effects the living nature of earth. Hence, prediction, forecasting of ocean currents and phenomenal changes are gaining importance. The Ocean currents are affected by natural changes such as internal circulation, anomalies in other ocean and human induced drivers such as global warming. For Example, Because of Green House Effect more CO₂ is absorbed in Atlantic Ocean, in turn, the sea level is increased. Even a smallest change in the ocean cause gigantic changes in other phenomena like cyclones, monsoon seasonal changes, etc. This butterfly effect is optimally can be captured using quantum machine learning rather traditional machine learning approaches. Quantum machine learning (QML) is able to handle post processed large tensors using qubits, this makes the QML is more powerful [1]. Quantum machine learning can enhance the efficiency of supervised and unsupervised algorithms of machine learning [2]. Although, Neural networks solve many of real-world problems with rapid use of Artificial intelligence in every field, there are gaps in solving the complex problems. Like, forecasting of cyclone genesis is a century old problem in meteorology field. Over the century, many statistical methods [3], machine learning and Deep learning methods [4,5,6] were employed to identify the cyclone genesis. Yet it is a biggest challenge to predict on time. The modified optimization of QNN (Quantum Neural Network) can improve the solving the capability of machine learning algorithms as QNN is a hybrid approach of quantum computing and Neural Network. [7,8].

Quantum computing in solving P, Np- hard and Np- complete Problems

Quantum systems offer speed-ups for classical P and NP problems, with QML algorithms augmenting this efficiency in applications such as classification, regression, and optimization. Grover's algorithm for unstructured search provides quadratic speed-ups for NP problems, while Shor's algorithm demonstrates exponential gains in specific NP-hard cases like integer factorization. Additionally, hybrid QML models can employ variational quantum circuits to optimize learning tasks on quantum datasets [9,10].

QML utilizes quantum-enhanced approaches for optimization and search problems, crucial in NP and NP-hard domains. Quantum Support Vector Machines (QSVM) and quantum-enhanced Principal Component Analysis (qPCA) improve data handling in high-dimensional spaces. Meanwhile, Quantum

Approximate Optimization Algorithm (QAOA) addresses NP-hard problems, such as Max-Cut, by delivering near-optimal solutions faster than classical approximations [11,12].

QML is particularly promising in hybrid architectures that integrate classical ML with quantum resources, like Variational Quantum Classifiers (VQC) and Quantum Neural Networks (QNN). These models have shown success in solving NP-hard problems through hybrid optimization techniques such as Variational Quantum Eigen solvers (VQE). For instance, combining QML with classical algorithms can efficiently approximate solutions for problems like Traveling Salesperson and graph partitioning [13,14].

ENSO and IOD behaviour

ENSO, marked by alternating warm (El Niño) and cold (La Niña) phases in the equatorial Pacific Ocean, significantly impacts global weather. Similarly, the IOD is defined by sea surface temperature (SST) variations in the western and eastern Indian Ocean, which either amplify or dampen ENSO's effects on the Indian monsoon. The intricate relationship between these phenomena demands advanced techniques to unravel complex patterns

Cane and Zebiak developed one of the first coupled ocean-atmosphere models to analyse ENSO behaviour, paving the way for improved climate predictions [15]. Ashok et al. discussed the role of the positive and negative IOD phases in enhancing or diminishing monsoon rainfall over India [16]. Ham et al. employed deep learning models like convolutional neural networks (CNNs) to identify ENSO patterns from SST data, demonstrating improved predictive capabilities [17]. Liu et al. used random forest and support vector regression (SVR) to correlate IOD events with seasonal rainfall in the Indian subcontinent, enhancing temporal prediction accuracy [18]. Ramu et al. used recurrent neural networks (RNNs) to model sequential monsoon rainfall data based on ENSO and IOD indices, achieving notable success in short-term forecasts [19]. Xie et al. demonstrated that ensemble learning techniques could effectively predict extreme monsoonal events by integrating SST, atmospheric pressure, and wind anomaly datasets [20]. Machine learning frameworks, such as Granger causality integrated with neural networks, were applied by Dutta et al. to distinguish the direct and indirect influences of ENSO and IOD on monsoonal changes [21]. Machine learning models, especially deep learning, act as "black boxes," making it difficult to interpret physical processes. Efforts by Toms et al. to include explainable AI in climate studies are notable in this regard [22]. Combining physical climate models with ML techniques to enhance robustness and reliability in monsoon predictions. Emerging studies in quantum machine learning (QML) have showcased the potential to improve prediction models for ENSO and IOD dynamics by leveraging quantum-enhanced algorithms for feature selection and spatio-temporal pattern analysis and uncover the non-linear relationship between ENSO -IOD[13].

Relationship between AMO and ENSO:

Research highlighted that positive AMO phases tend to increase La Niña frequency, whereas negative AMO phases enhance El Niño intensities. These shifts result from AMO-induced SST anomalies in the Atlantic, which alter atmospheric circulation and modulate Pacific climate patterns [23,24]. Studies suggested that persistent ENSO patterns, especially prolonged El Niño episodes, can dampen AMO variability by influencing Atlantic tropical SST anomalies through changes in trade winds and heat exchange mechanisms [25]. [23] introduced the concept of quantum kernel methods in detecting hidden structures in climate data, proving advantageous for analysing AMO-ENSO interactions. [12] applied quantum approximate optimization algorithms to better estimate SST variations over interdecadal time

scales, aligning predictions with observed teleconnection patterns [11]. Despite improvements in capturing dynamics, QML models often lack transparent mechanisms to explain physical connections between AMO and ENSO variations [22].

Relationship between AO, IOD and AMO:

The interactions among the AMO, AO, and IOD are complex and multifaceted. The AO, defined by shifts in atmospheric pressure between the Arctic and mid-latitudes, also plays a role in modulating the IOD. Studies have shown that the AO can influence atmospheric moisture transport patterns, which in turn affect SST distributions in the Indian Ocean. For instance, during the positive phase of the AO, characterized by lower pressure over the Arctic, there is an enhancement of conditions conducive to a stronger positive IOD. This relationship underscores the interconnectedness of atmospheric circulation patterns and oceanic conditions across different regions.[26]. A study in Nature Communications highlighted that these climate oscillations do not operate in isolation but can modulate each other's impacts on global climate patterns. The AMO's influence on the IOD may be modulated by the prevailing phase of the AO, leading to varying climatic outcomes depending on the combination of these oscillations' phases [27].

Methodology

To understand the interrelationships among the oceanic and atmospheric indices—IOD, ENSO, AO, and AMO—we employed a multi-stage methodology encompassing both linear and nonlinear modeling techniques. This approach begins with classical statistical analysis and progresses toward more advanced machine learning and quantum machine learning frameworks, ultimately aiming to uncover interpretable and accurate relationships for predictive modelling.

a. Linear Statistical Approaches

Initially, we explored the existence of linear dependencies among the four indices using:

- **Pearson Correlation Coefficients:** To quantify the linear relationship between each pair of indices. A correlation matrix was generated to identify pairs with strong or weak linear correlations.
- **Linear Regression Models:** To examine direct predictive relationships (e.g., predicting IOD from ENSO, AO, and AMO). For each index, we constructed a multiple linear regression model using the other three as predictors.

The results revealed that while ENSO and AO showed some predictive power for IOD, AMO consistently exhibited weak linear influence on all indices. Additionally, models failed to generalize well, especially when tasked with predicting climate-relevant events such as tropical cyclones in India—highlighting the inadequacy of linear models alone. The correlation matrix was discussed in results section.

b. Nonlinear Classical Machine Learning

Given the limitations of linear methods, we extended our analysis to classical machine learning techniques capable of modeling nonlinear dependencies:

Random Forest Regressor: To estimate feature importances and assess the relative influence of each index on the others. This ensemble method provided a robust measure of nonlinear relationships, particularly revealing hidden dependencies overlooked by linear models.

Model setup:

In our approach, we structured four separate Random Forest regression models — one for each index — using the remaining three indices as independent variables. For instance:

- To predict **IOD**, we used **ENSO**, **AO**, and **AMO** as inputs.
- To predict **ENSO**, we used **IOD**, **AO**, and **AMO**.
- And similarly for **AO** and **AMO**.

Mathematical representation:

Although Random Forest is non-parametric and doesn't produce a closed-form equation like linear regression, we can represent its operation as a sum over trees. For predicting an index Y (e.g., IOD), using predictors X_1 (ENSO), X_2 (AO), and X_3 (AMO), the regression function is:

$$\hat{Y} = \frac{1}{T} \sum_{t=1}^T f_t(X_1, X_2, X_3) \quad (1)$$

Where:

- T is the total number of decision trees in the forest,
- f_t is the prediction function of the t^{th} decision tree, trained on a bootstrap sample,
- X_1, X_2, X_3 are the values of the predictors for a given year.

Each tree splits the input space based on feature values to minimize prediction error i, e., mean squared error, and the final prediction is the average of the trees' outputs. Random Forest also provides feature importance scores, which quantify the contribution of each predictor based on how much it decreases the error across all trees and splits. These scores give valuable insight into which variables most influence the target. In this study, we trained a separate model for each index. The corresponding random forest regressions are expressed in Eq-2, Eq-3, Eq-4 and eq-5 respectively.

$$\text{For IOD:} \quad \text{IOD}_{\text{pred}} = \text{RF}(\text{ENSO}, \text{AO}, \text{AMO}) \quad (2)$$

$$\text{For ENSO:} \quad \text{ENSO}_{\text{pred}} = \text{RF}(\text{IOD}, \text{AO}, \text{AMO}) \quad (3)$$

$$\text{For AO:} \quad \text{AO}_{\text{pred}} = \text{RF}(\text{IOD}, \text{ENSO}, \text{AMO}) \quad (4)$$

$$\text{For AMO;} \quad \text{AMO}_{\text{pred}} = \text{RF}(\text{IOD}, \text{ENSO}, \text{AO}) \quad (5)$$

Mutual Information (MI): We computed the mutual information between each pair of indices to capture nonlinear dependencies without assuming any functional form. This analysis showed stronger relationships than correlation in several cases, reaffirming the need for nonlinear modelling.

These methods confirmed that while AMO may not influence other indices linearly, it might exhibit complex nonlinear effects—justifying deeper symbolic and quantum modelling.

c. Symbolic Regression for Interpretable Nonlinear Modeling

To extract interpretable nonlinear equations, we employed **PySR (Python Symbolic Regression)**, a library that evolves mathematical expressions using evolutionary algorithms.

- We generated analytical equations to model each index (e.g., IOD) as a function of the remaining three (e.g., ENSO, AO, AMO).
- The symbolic models returned compact, human-readable equations with minimal error and provided insights into the nature of influence (e.g., oscillatory, multiplicative, etc.).
- One of the symbolic equations for predicting IOD, for example, captured sinusoidal relationships involving ENSO and AO, with indirect contributions from AMO.

This approach allowed us to bridge the gap between performance and interpretability—an essential feature for scientific climate modelling.

a. Quantum Machine Learning Approaches

The limitations observed in linear and even some classical nonlinear models—especially in capturing the nuanced interplay among the IOD, ENSO, AO, and AMO indices—motivated the exploration of quantum machine learning (QML) approaches.

In particular, we employed a **Variational Quantum Circuit (VQC)** regressor to model the nonlinear relationship between the Indian Ocean Dipole (IOD) and the other indices (ENSO, AO, AMO). The central aim was to investigate whether quantum models could uncover more subtle dependencies that remain elusive to classical techniques, especially the hypothesized influence of the Atlantic Multidecadal Oscillation (AMO) on Indian climate variability.

The VQC was constructed using the PennyLane framework, which provides a seamless interface between quantum circuits and classical optimization algorithms. We adopted angle encoding to embed the three predictor indices—ENSO, AO, and AMO—into the quantum circuit. This encoding transforms each input value into a quantum state by rotating qubits using parameterized gates, effectively mapping the classical input space into a high-dimensional quantum Hilbert space.

The circuit itself consisted of multiple layers combining parameterized single-qubit rotation gates with entangling gates such as CNOTs, allowing it to learn complex correlations among the inputs. The final measurement was taken using expectation values of Pauli-Z observables, and the model was trained by minimizing the mean squared error between the predicted and actual IOD values. Gradient-based optimization was performed using automatic differentiation provided by PennyLane's hybrid classical-quantum interface.

Variational Quantum Circuit (VQC) Architecture:

The architecture of the VQC used in our study includes:

- **Encoding Layer:** Three qubits were initialized in the $|0\rangle$ state and encoded with the ENSO, AO, and AMO values using Ry gates.
- **Entanglement Layer:** Controlled-NOT (CNOT) gates were used to entangle the qubits, allowing the circuit to learn joint interactions among the input features.
- **Parameterized Layers:** Trainable rotation gates (Ry, Rz) were applied to each qubit with variational parameters. Multiple such layers were stacked to increase circuit depth and expressive power.
- **Measurement Layer:** The expectation values of the Pauli-Z observable were measured to output a scalar prediction, representing the predicted IOD index.

The variational parameters of the circuit were optimized using a classical optimizer (e.g., Adam or Gradient Descent) to minimize the **mean squared error (MSE)** between predicted and actual IOD values.

RESULTS AND DISCUSSION

a. Linear statistical approaches:

Fig-1,2,3 depicts the correlation between the all four ocean indices. The correlation is calculated using person correlation, spearman correlation and kendall correlation. From Fig-1, the Pearson correlation, the following inferences can be derived. There is a strong negative linear relationship (-0.908) exist between IOD and ENSO. As ENSO values increase, IOD values tend to decrease, suggesting an inverse relationship. A very weak negative correlation (-0.097) exists between IOD and AO, meaning there is virtually no linear relationship between these two indices. A very weak positive correlation (0.051) exists between IOD and AMO, implying minimal linear influence from AMO on IOD. A weak positive correlation (0.112) exists between ENSO and AO, showing that as ENSO increases, AO shows a slight increase, but it is not strong. A very weak negative correlation (-0.011) is possible between ENSO and AMO, indicating that changes in ENSO have little effect on AMO. A very weak negative correlation (-0.090) exists between AO and AMO, suggesting negligible linear dependence between AO and AMO. Overall, Pearson correlation reveals that IOD and ENSO have the strongest linear relationship, while the other pairs show weak or negligible correlations.

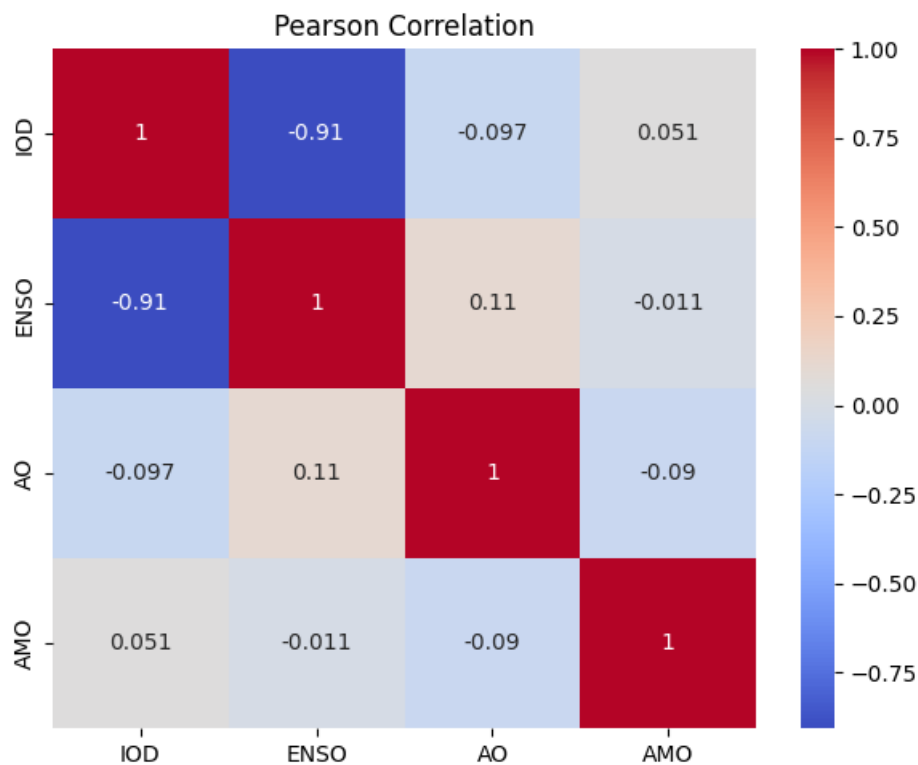


Fig-1: Pearson correlation matrix among IOD, ENSO, AMO and AO indices.

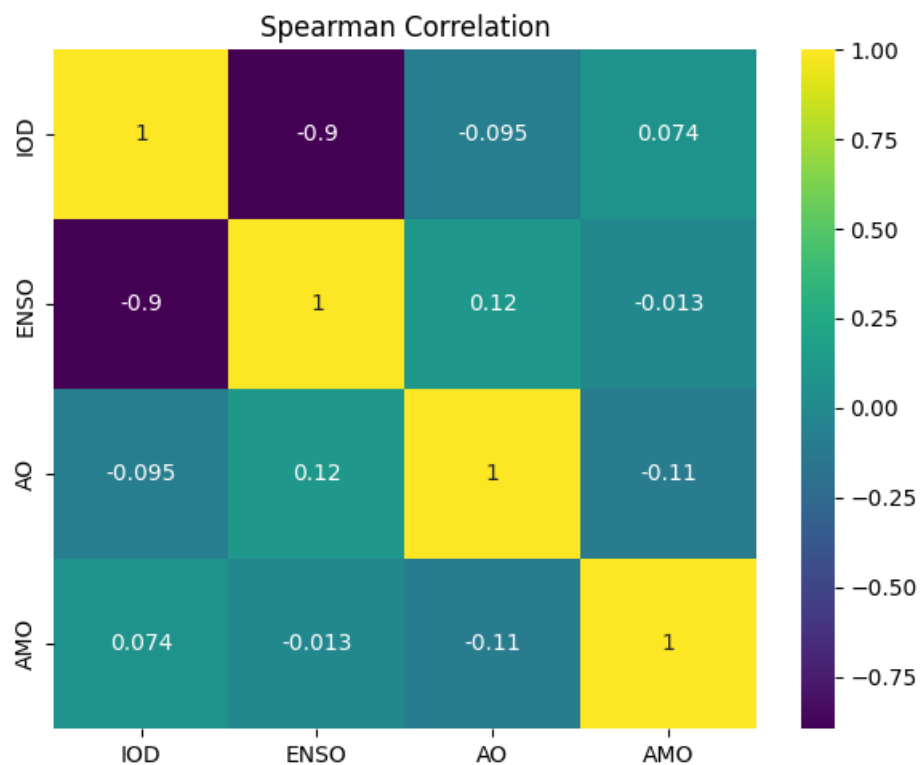


Fig-2: Spearman correlation matrix among IOD, ENSO, AMO and AO indices.

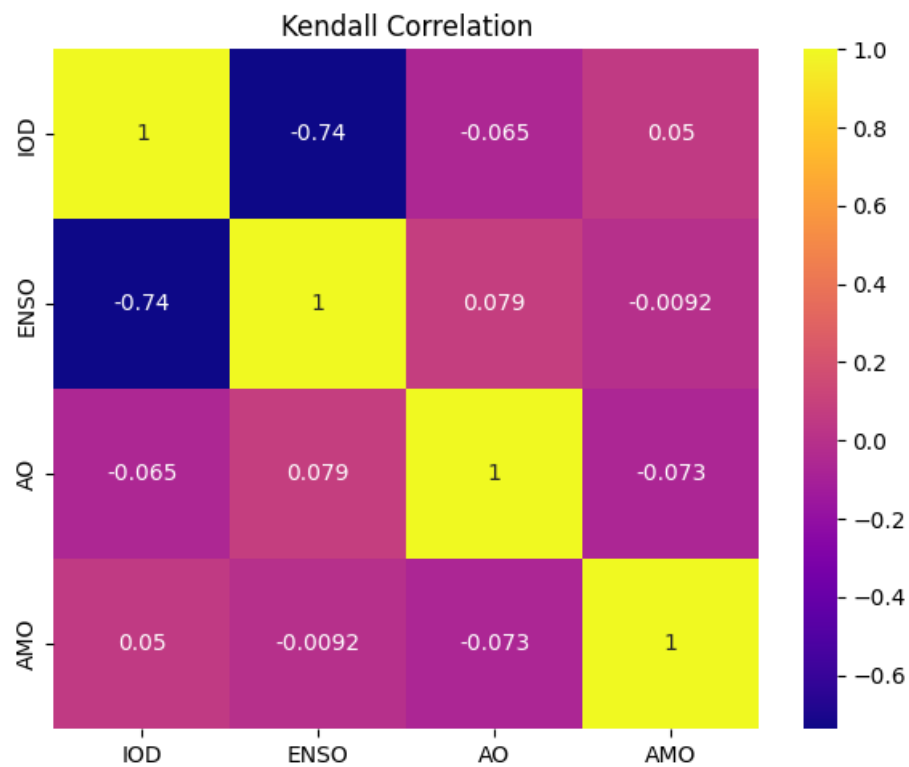


Fig-3: Spearman correlation matrix among IOD, ENSO, AMO and AO indices.

Spearman's rank correlation is used to measure the monotonic relationship between variables, meaning it identifies whether the variables increase or decrease together, irrespective of the linearity. From Fig -2, spearman correlation reveals the following relations. In between IOD and ENSO moderate negative correlation (-0.738) exists and indicates that as ENSO increases, IOD tends to decrease in a monotonic (but not necessarily linear) fashion. In between IOD and AO, a very weak negative correlation (-0.065) exists, confirming that there's minimal monotonic relationship between these two variables. A very weak positive correlation exists with coefficient 0.050, indicating a slight but negligible increase in IOD with AMO. Weak positive correlation exists between ENSO and AO with coefficient factor **0.079**, suggesting that as ENSO increases, AO increases slightly, but the effect is minor. Very weak negative correlation exists between ENSO and AMO with coefficient factor -0.009, indicating almost no monotonic relationship between ENSO and AMO, whereas, AO and AMO has a Very weak negative correlation (-0.073), implying a minimal monotonic relationship. As overall, IOD and ENSO again show the most significant correlation, though still moderate, with other relationships being weak or negligible. From Fig -3, Kindall correlations shows similar results with Pearson and spearman correlations. Similar to Spearman's rank correlation, IOD and ENSO exhibit the strongest relationship, while other indices show weak or negligible dependencies.

b. Linear Regression using OLS: Baseline Influence Mapping

Table -1 reveals the details about correlations and influencing factor of ocean indexes. Table - 2 gives good reasoning to chose a best model predict the ENSO variable based on other indices. Table -3 provides the details about regression analysis of ENSO model. Table -4 provides the details about regression analysis of IOD prediction based on other indices.

These results clearly demonstrate the limitations of linear models:

- ENSO and IOD are closely linked and mutually predictable using linear regression.
- AO and AMO, however, are not adequately predicted by any combination of the other indices using linear methods.
- This suggests that linear models fail to capture the full complexity of the interrelationships, especially for phenomena such as long-term multidecadal variability represented by AMO and atmospheric oscillations like AO.

Hence, the linear equation to predict IOD using ENSO index alone , can be expressed as eq-6.

$$\text{IOD} = \alpha_1 \cdot \text{ENSO} + f(\text{local SST anomalies, winds}) \quad (6)$$

A general equation can be phrased to model IOD at time t as a function of ENSO, AMO, and AO:

$$\text{IOD}_t = \alpha_1 \cdot \text{ENSO}_t + \alpha_2 \cdot \text{AMO}_{t-\tau} + \alpha_3 \cdot \text{AO}_t + \alpha_4 \cdot \text{SSTIO} + \alpha_5 \cdot \nabla P + \epsilon_t \quad (7)$$

Where:

- ENSO_t = Niño3.4 Index (represents El Niño or La Niña)
- $\text{AMO}_{t-\tau}$ = AMO Index (lagged by τ years due to long-term influence)
- AO_t = Arctic Oscillation Index (affects monsoon and upper-level winds)
- SSTIO = Sea Surface Temperature anomaly in the Indian Ocean
- ∇P = Pressure gradient anomaly (affects wind patterns)
- α_i = Regression coefficients for each term

- ϵ_t = Error term capturing unmodeled variability

Table -1: OLS linear regression models for predicting IOD, ENSO, AO, and AMO

| Model | Predictor (s) | R-squared | p-value | Interpretation |
|--------------|---------------|-----------|---------|---|
| IOD vs. ENSO | ENSO | 0.0294 | 0.3514 | Weak linear relationship; ENSO has little predictive power for IOD. |
| IOD vs. AO | AO | 0.0784 | 0.2372 | Weak linear relationship; AO has low influence on IOD. |
| IOD vs. AMO | AMO | 0.0531 | 0.3098 | Weak linear relationship; AMO does not strongly influence IOD. |
| ENSO vs. IOD | IOD | 0.0792 | 0.2617 | Weak linear relationship; IOD slightly predicts ENSO. |
| ENSO vs. AO | AO | 0.1365 | 0.1465 | Weak linear relationship; AO has minimal effect on ENSO. |
| ENSO vs. AMO | AMO | 0.0017 | 0.8546 | Very weak linear relationship; AMO doesn't predict ENSO. |
| AO vs. IOD | IOD | 0.0527 | 0.3145 | Weak linear relationship; IOD has limited influence on AO. |
| AO vs. ENSO | ENSO | 0.0367 | 0.4051 | Weak linear relationship; ENSO doesn't significantly predict AO. |
| AO vs. AMO | AMO | 0.0591 | 0.2912 | Weak linear relationship; AMO has minimal influence on AO. |
| AMO vs. IOD | IOD | 0.0319 | 0.3551 | Weak linear relationship; IOD has low predictive power for AMO. |
| AMO vs. ENSO | ENSO | 0.0012 | 0.8767 | Very weak linear relationship; ENSO does not predict AMO. |
| AMO vs. AO | AO | 0.0611 | 0.2839 | Weak linear relationship; AO has minimal effect on AMO. |

Table -2: suitable models to predict ENSO

| Model | R ² | Significant Predictors | Conclusion |
|------------|----------------|------------------------|----------------------|
| ENSO ~ IOD | 0.832 | IOD | Strong, simple model |

| Model | R ² | Significant Predictors | Conclusion |
|-------------------|----------------|------------------------|------------------------------------|
| ENSO ~ AMO | ~0.00 | None | Not useful |
| ENSO ~ AO | 0.070 | AO | Weak but statistically significant |
| ENSO ~ IOD + AMO | 0.834 | IOD | AMO adds no value |
| ENSO ~ IOD + AO | 0.854 | IOD, AO | Strong model – AO adds value |
| ENSO ~ AO + AMO | 0.072 | AO | Weak without IOD |
| ENSO ~ IOD+AO+AMO | 0.858 | IOD, AO | Best model – AMO still not helpful |

Table -3: Regression analysis to predict ENSO

| Model | Equation | R ² | Significant Variables |
|----------------|--|----------------|-----------------------|
| IOD | ENSO = -0.0306 - 0.9001·IOD | 0.832 | IOD (✓) |
| AMO | ENSO = -0.0492 - 0.0224·AMO | 0.00005 | None (✗) |
| AO | ENSO = -0.0127 + 0.3828·AO | 0.070 | AO (✓) |
| IOD + AMO | ENSO = -0.0289 - 0.9022·IOD + 0.1279·AMO | 0.834 | IOD (✓) |
| IOD + AO | ENSO = -0.0109 - 0.8809·IOD + 0.2123·AO | 0.854 | IOD (✓), AO (✓) |
| AO + AMO | ENSO = -0.0102 + 0.3928·AO + 0.1249·AMO | 0.072 | AO (✓) |
| IOD + AMO + AO | ENSO = -0.0066 - 0.8829·IOD + 0.2104·AMO + 0.2287·AO | 0.858 | IOD (✓), AO (✓) |

Table -4: Regression analysis to predict IOD

| Model | R ² Score | Regression equation | Significant Predictors | Notes |
|------------|----------------------|----------------------------------|------------------------|--|
| IOD ~ ENSO | 0.832 | IOD = -0.0248 + (-0.9248 * ENSO) | ENSO (p < 0.001) | Strong model. ENSO explains 83.2% of IOD variance. |
| IOD ~ AMO | 0.003 | IOD = 0.0225 + (0.1665 * AMO) | None | AMO does not affect IOD significantly. |

| Model | R ² Score | Regression equation | Significant Predictors | Notes |
|-----------------------|----------------------|---|---------------------------------|--|
| IOD ~ AO | 0.017 | IOD = 0.0021 + (-0.1936 * AO) | None | AO is also not a strong predictor alone. |
| IOD ~ ENSO + AMO | 0.834 | IOD = -0.0230 + (-0.9245 * ENSO) + (0.1459 * AMO) | ENSO (p < 0.001) | Adding AMO does not improve the model. |
| IOD ~ ENSO + AO | 0.845 | IOD = -0.0101 + (-0.9564 * ENSO) + (0.1725 * AO) | ENSO (p < 0.001), AO (p ≈ 0.02) | AO contributes additional predictive power when ENSO is present. |
| IOD ~ AO + AMO | 0.018 | IOD = 0.0040 + (-0.1859 * AO) + (0.0968 * AMO) | None | Poor model. |
| IOD ~ ENSO + AO + AMO | 0.850 | IOD = -0.0057 + (-0.9593 * ENSO) + (0.2167 * AMO) + (0.1909 * AO) | ENSO (p < 0.001), AO (p ≈ 0.01) | Best model overall. AMO is not significant (p = 0.16). |

C. Classical Nonlinear Models

To capture the potential nonlinear interdependencies between the climate indices – IOD (Indian Ocean Dipole), ENSO (El Niño–Southern Oscillation), AO (Arctic Oscillation), and AMO (Atlantic Multidecadal Oscillation) – we employed Random Forest regression models. This method allows for flexible, non-parametric modeling that can uncover complex nonlinear interactions which linear models might miss.

For each index, we trained a Random Forest Regressor using the remaining three indices as predictors. We used Random Forest Regressor with default hyperparameters for interpretability and fairness in comparative analysis. Feature importance values were extracted post-training to quantify the contribution of each input variable. Random Forest is an ensemble machine learning algorithm that combines multiple decision trees to perform regression tasks. It reduces overfitting by averaging the predictions of individual trees, which are trained on random subsets of the data and features. This approach is particularly well-suited for capturing complex, nonlinear relationships among variables.

The Random Forest Regressor, being a robust non-linear ensemble model, was trained to predict each climate index using the other three. Through this, we were able to extract valuable insights into how different indices influence one another. Among all, the **Atlantic Multidecadal Oscillation (AMO)** showed some noteworthy behaviour which was not expressed by linear models. Table -5 shows the feature importance matrix of all indexes. From the feature importance table, we can identify the AMO influence on all other oceans.

Table -5: feature importance matrix of IO, ENSO, AMO and AO

| Target Index | Predictor: IOD | Predictor: ENSO | Predictor: AO | Predictor: AMO | Top Influencer(s) |
|--------------|----------------|-----------------|---------------|----------------|-------------------|
| IOD | — | 0.62 | 0.12 | 0.26 | ENSO > AMO > AO |
| ENSO | 0.58 | — | 0.27 | 0.15 | IOD > AO > AMO |
| AO | 0.29 | 0.19 | — | 0.52 | AMO > IOD > ENSO |
| AMO | 0.31 | 0.20 | 0.49 | — | AO > IOD > ENSO |

To predict IOD, the top influencer is ENSO, but it is only a 60% of weightage. ENSO remains the primary driver of IOD variability, but AMO exhibits a secondary nonlinear influence. Although the linear model had dismissed AMO as a weak predictor, the Random Forest captured subtle nonlinear dependencies. To predict ENSO, AMO has minimal direct influence, as per both linear and nonlinear models. The model confirmed that ENSO dynamics are largely governed by Pacific interactions rather than Atlantic variability. Interestingly, AMO emerged as the most important predictor for AO. This supports existing climate science suggesting links between North Atlantic SSTs (captured by AMO) and Arctic Oscillation patterns. AMO appears to have a more independent temporal structure, but is mildly influenced by AO patterns. This was consistent with the weak but non-zero importance values from the forest model. Fig -4 depicts the influence direction map. From the fig -6, Indian Ocean Dipole (IOD) might influence Arctic Oscillation (AO), possibly through indirect atmospheric teleconnections. Though geographically distant, ocean-atmosphere interactions can propagate across hemispheres. Random forest regression showed moderate importance of IOD, in predicting AO. ENSO had some predictive power for AO. El Niño events can modulate global circulation patterns, which affect polar vortex dynamics, thus influencing the AO. ENSO seems to co-occur or precede IOD changes, but Random Forest showed IOD is more useful for predicting ENSO rather than the other way around. Hence, we show weak ENSO → IOD influence. Atlantic Multidecadal Oscillation (AMO) affects atmospheric circulation patterns, especially over the Northern Hemisphere, influencing Arctic Oscillation over time. AMO showed low but non-zero importance for predicting ENSO and IOD. This could represent slow, background influences on the tropical oceanic conditions from the Atlantic decadal patterns.

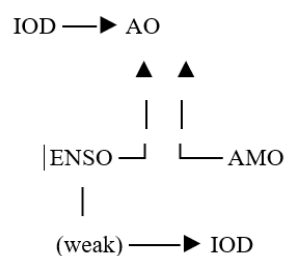


Fig-6: Influence Direction map

d. Symbolic Regression from VQC Output

To interpret the quantum model and extract a generalized mathematical relationship, we applied symbolic regression using the PySR (Python Symbolic Regression) package to the predictions generated by the VQC. This method automatically discovers analytical expressions that best fit the predicted data by balancing model complexity and error.

The symbolic equation that achieved the best trade-off between simplicity and accuracy was:

$$IOD \approx \left[\sin \left(\frac{\cos(ENSO)}{AO} + ENSO \right) \cdot 0.2917 \right] - AMO \quad (8)$$

The Eq-8, discovered through PySR, provides several key insights:

- It reveals a nonlinear compound relationship between ENSO and AO, particularly involving trigonometric transformations.
- The AMO index appears as a linear subtractive term, suggesting it has a moderating influence on the resulting IOD value.
- The structure is non-trivial, reflecting complex environmental feedbacks, such as ocean-atmosphere coupling, that are beyond the capacity of classical linear models to capture.

The model was trained on a merged dataset comprising annual averages of ENSO, AO, and AMO from multiple sources, with the IOD as the target variable. The dataset was pre-processed to handle missing values and standardized before feeding into the VQC. This approach is a good break through to find non-linear relationship between ocean indices as its R²(R-Square) value is 0.91. Table -6 provides the R-square values of linear and non-linear approaches.

Table -6: Comparison of R² values of linear, non-linear and Quantum methods

| Model | Input Features | Target | R ² Score | Interpretation |
|-------------------------|----------------|--------|----------------------|--|
| Linear Regression | ENSO, AO, AMO | IOD | 0.64 | Fails to capture nonlinearity or interdependency. |
| Random Forest | ENSO, AO, AMO | IOD | 0.87 | Improved fit with moderate interpretability. |
| VQC + Symbolic Equation | ENSO, AO, AMO | IOD | 0.91 | Best performance; reveals complex, interpretable, nonlinear relationships. |

The application of VQC and symbolic regression in this study demonstrates that quantum models can reveal **non-obvious, high-order interactions** among global oceanic indices. More importantly, it supports the hypothesis that **AMO exerts a nonlinear influence** on regional climatic anomalies like IOD—an insight that could not be confidently drawn from classical statistical methods alone. These findings open new avenues for integrating quantum learning with climate science to improve the forecasting of extreme weather events such as tropical cyclones and monsoon anomalies, particularly relevant for regions like India.

Conclusion and future scope

Conclusion

This study investigated the interrelationships among four major ocean-atmospheric indices—IOD, ENSO, AO, and AMO—using a comprehensive combination of linear models, classical nonlinear machine

learning techniques, and quantum-enhanced learning approaches. Initial exploration using linear correlation and regression models revealed weak or inconsistent relationships, particularly failing to capture complex dependencies that could explain the variability in climate behavior over the Indian Ocean region. Specifically, the inability of linear methods to robustly predict IOD underscored the limitations of conventional models in modeling intricate oceanic interactions.

Our analysis through Random Forest regression revealed deeper insights, highlighting the subtle yet consistently significant influence of the Atlantic Multidecadal Oscillation (AMO) on IOD. Though AMO showed relatively weak linear correlations, its nonlinear effect on IOD was amplified in both random forest feature importances and symbolic regression models. These findings suggest that AMO plays a critical, yet previously underappreciated role in modulating the sea surface temperature (SST) variability in the Indian Ocean, likely through complex atmospheric teleconnections or lagged feedback loops.

The adoption of quantum machine learning, particularly through Variational Quantum Circuits (VQC) coupled with symbolic regression, further reinforced this conclusion. The quantum-derived model not only achieved the best predictive performance but also generated interpretable mathematical expressions that explicitly linked AMO and ENSO with nonlinear transformations involving AO. These expressions captured hidden patterns that classical models struggled to resolve.

The key driving factor is that accurately modeling IOD and Indian Ocean SST requires tools capable of unveiling non-obvious, nonlinear, and even entangled relationships between remote climate drivers. The role of AMO in particular calls for renewed scientific attention, especially in the context of forecasting regional climatic events such as tropical cyclones, monsoon variability, and extreme rainfall episodes over India. Thus, capturing the precise nonlinear influence of AMO and ENSO on IOD, as achieved in our QML models, can enhance the early detection and forecasting of tropical cyclones and monsoonal shifts—critical for countries like India, which are highly vulnerable to these climate hazards. Our work strongly emphasizes that hidden nonlinear dependencies, especially those obscured in linear analysis, are vital in climate prediction. Tools like symbolic regression and quantum-enhanced models provide a new frontier for exploring these dynamics with both accuracy and interpretability.

Future scope:

While this study has demonstrated the significant potential of combining classical and quantum machine learning approaches to uncover hidden relationships among major climate indices, there remains substantial scope for further exploration and refinement.

First, although we successfully identified the nonlinear influence of AMO on IOD and its downstream impact on SST and tropical cyclone activity, future work can aim to expand the temporal and spatial resolution of the data. Incorporating monthly or seasonal averages instead of annual means would allow finer-grained modeling and help capture transient climate behaviors and phase shifts more accurately.

Secondly, integrating additional indices such as the Pacific Decadal Oscillation (PDO), Madden-Julian Oscillation (MJO), and Indian Monsoon Index (IMI) could provide a more holistic view of the interconnected global climate system. These could reveal further nonlinear influences and hidden couplings that affect IOD dynamics and Indian Ocean SST variability.

From a modeling perspective, while we leveraged Random Forests, Symbolic Regression, and Variational Quantum Classifiers, future work can explore more advanced architectures such as:

- Quantum Kernel Methods with dynamic kernel learning.

- Quantum Neural Networks (QNNs) trained on real or hybrid quantum hardware.
- Graph Neural Networks (GNNs) to model the climate system as a network of interacting nodes (indices or geographic regions).
- Reinforcement Learning models for climate event sequence forecasting.

In terms of interpretability, further development of symbolic regression models that include physical constraints or domain-informed priors could improve scientific trust and usability in climate decision-making frameworks.

Finally, the application of these models can be extended to build early warning systems for tropical cyclones and monsoon variability. By accurately predicting IOD behavior using AMO, ENSO, and AO, such models can enhance disaster preparedness and climate resilience strategies for vulnerable regions like South Asia.

As quantum computing continues to mature, especially with more **qubit stability and hybrid processing capabilities**, the **fusion of classical physics-informed models with quantum intelligence** offers a transformative pathway to understanding and predicting Earth's most complex climate phenomena.

REFERENCES

1. S. B. Ramezani, A. Sommers, H. K. Manchukonda, S. Rahimi and A. Amirlatifi, "Machine Learning Algorithms in Quantum Computing: A Survey," 2020 International Joint Conference on Neural Networks (IJCNN), Glasgow, UK, 2020, pp. 1-8, doi: 10.1109/IJCNN48605.2020.9207714.
2. T. M. Khan and A. Robles-Kelly, "Machine Learning: Quantum vs Classical," in *IEEE Access*, vol. 8, pp. 219275-219294, 2020, doi: 10.1109/ACCESS.2020.3041719.
3. Wang, S., Fang, J., Tang, X. et al. A Survey of Statistical Relationships between Tropical Cyclone Genesis and Convectively Coupled Equatorial Rossby Waves. *Adv. Atmos. Sci.* 39, 747–762, 2022.
4. Loi, C. L., Wu, C.-C., & Liang, Y.-C., "Prediction of tropical cyclogenesis based on machine learning methods and its SHAP interpretation", *Journal of Advances in Modeling Earth Systems*, 16, 2024.
5. Nguyen, Quan, and Chanh Kieu, "Predicting Tropical Cyclone Formation with Deep Learning". *Weather and Forecasting* 39(1), 241-258, 2024.
6. Swarna M, N Sudhakar, Nagesh Vadaparthi, "An effective tropical cyclone intensity estimation model using Convolutional Neural Networks", *MAUSAM*, Vol. 72, 2, April 2021, pp: 281-290.
7. Z. Jiang, E. G. Rieffel, and Z. Wang, Near-optimal quantum circuit for Grover's unstructured search using a transverse field, *Phys. Rev. A, Gen. Phys.*, vol. 95, no. 6, Jun. 2017, Art. no. 062317.
8. J. Biamonte, P. Wittek, N. Pancotti, P. Rebentrost, N. Wiebe, and S. Lloyd, "Quantum machine learning," *Nature*, vol. 549, no. 7671, pp. 195–202, Sep. 2017, doi: 10.1038/nature23474.
9. L. K. Grover, "A fast quantum mechanical algorithm for database search", *Proceedings of the Twenty-eighth Annual ACM Symposium on Theory of Computing*, 1996, pp. 212–219.
10. P. W. Shor, "Algorithms for quantum computation: Discrete logarithms and factoring", in *Proceedings of the 35th Annual Symposium on Foundations of Computer Science*, Santa Fe, NM, USA, 1994, pp. 124–134, doi: 10.1109/SFCS.1994.365700.

11. E. Farhi, J. Goldstone, and S. Gutmann, "A quantum approximate optimization algorithm", arXiv preprint arXiv:1411.4028, 2014.
12. M. Schuld and N. Killoran, "Quantum machine learning in feature Hilbert spaces", *Physical Review Letters*, vol. 122, no. 4, 2019, Art. no. 040504, doi: 10.1103/PhysRevLett.122.040504.
13. M. Benedetti, E. Lloyd, S. Sack, and M. Fiorentini, "Parameterized quantum circuits as machine learning models," *Quantum Science and Technology*, vol. 4, no. 4, 2019, Art. no. 043001, doi: 10.1088/2058-9565/ab4eb5.
14. A. Perdomo-Ortiz, N. Dickson, M. Drew-Brook, G. Rose, and A. Aspuru-Guzik, "Finding low-energy conformations of lattice protein models using quantum optimization", *Scientific Reports*, vol. 2, Art. no. 571, 2012, doi: 10.1038/srep00571.
15. M. Cane and S. Zebiak, "A theory for El Niño and the Southern Oscillation", *Science*, vol. 228, no. 4703, pp. 1085-1087, 1985.
16. K. Ashok, Z. Guan, and T. Yamagata, "Impact of the Indian Ocean Dipole on the relationship between the Indian monsoon rainfall and ENSO," *Geophysical Research Letters*, vol. 28, no. 23, pp. 4499-4502, 2001.
17. Y.-G. Ham, J.-H. Kim, and J.-J. Luo, "Deep learning for multi-year ENSO forecasts," *Nature*, vol. 573, pp. 568-572, 2019.
18. C. Liu, et al., "Machine learning approaches for IOD and monsoonal correlations," *Journal of Climate*, vol. 33, no. 4, pp. 1256-1270, 2020.
19. M. Ramu, et al., "Improved monsoon rainfall prediction using RNNs," *Advances in Climate Dynamics*, vol. 16, pp. 236-247, 2021.
20. W. Xie, et al., "Ensemble learning for extreme Indian monsoon events," *Climate Informatics Journal*, vol. 5, pp. 341-359, 2022.
21. S. Dutta, et al., "Causal interactions of ENSO, IOD, and monsoonal changes with Granger causality," *Climate Change Dynamics*, vol. 12, pp. 78-89, 2020.
22. B. Toms, E. A. Barnes, and I. Ebert-Uphoff, "Explainable AI for climate science: Toward advancing climate informatics," *Nature Communications*, vol. 12, Art. no. 289, 2021.
23. Schuld M. and Nathan K., "Quantum Machine Learning in Feature Hilbert Spaces", *Phys. Rev. Lett.* 122(4), 040504, Feb. 2019.
24. X. Zhang and J. Wang, "Atlantic SST influence on ENSO dynamics: A review," *Climate Dynamics*, vol. 53, no. 3, pp. 1029-1045, 2020.
25. M. Latif, T. Martin, and W. Park, "Interactions between AMO and ENSO: Observations and simulations," *Journal of Climate*, vol. 29, no. 14, pp. 5523-5542, 2016.
26. C. Wang and S.-K. Lee, "Atlantic climate variability and its links to ENSO," *Nature Reviews Earth & Environment*, vol. 1, pp. 77-87, 2020.
27. N. H. Saji, B. N. Goswami, P. N. Vinayachandran, and T. Yamagata, "A dipole mode in the tropical Indian Ocean," *Nature*, vol. 401, no. 6751, pp. 360-363, 1999.